Steel and Composite Structures, *Vol. 33, No. 5* (*2019*) *717-727*
DOI: https://doi.org/10.12989/scs.2019.33.5.717

Using IGA and trimming approaches for vibrational analysis of L-shape graphene sheets via nonlocal elasticity theory

Vahid Tahouneh*, Mohammad Hasan Naei and Mahmoud Mosavi Mashhadi

School of Mechanical Engineering, *College of Engineering*, *University of Tehran*, *Tehran*, *Iran*

(*Received July 25, 2019, Revised October 16, 2019, Accepted October 21, 2019*)

Abstract. This paper is motivated by the lack of studies in the technical literature concerning to vibration analysis of a single-layered graphene sheet (SLGS) with corner cutout based on the nonlocal elasticity model framework of classical Kirchhoff thin plate. An isogeometric analysis (IGA) based upon non-uniform rational B-spline (NURBS) is employed for approximation of the L-shape SLGS deflection field. Trimming technique is employed to create the cutout in geometry of L-shape plate. The L-shape plate is assumed to be Free (F) in the straight edges of cutout while any arbitrary boundary conditions are applied to the other four straight edges including Simply supported (S), Clamped (C) and Free (F). The Numerical studies are carried out to express the influences of the nonlocal parameter, cutout dimensions, boundary conditions and mode numbers on the variations of the natural frequencies of SLGS. It is precisely shown that these parameters have considerable effects on the free vibration behavior of the system. In addition, numerical results are validated and compared with those achieved using other analysis, where an excellent agreement is found. The effectiveness and the accuracy of the present IGA approach have been demonstrated and it is shown that the IGA is efficient, robust and accurate in terms of nanoplate problems. This study serves as a benchmark for assessing the validity of numerical methods used to analyze the single-layered graphene sheet with corner cutout.

Keywords: single-layered graphene sheet; free vibration; isogeometric analysis; trimming technique; NURBS; L-shape structure

1. Introduction

Indubitable, one of the most significant allotropes of carbon is graphene containing a single layer of carbon atoms organized in a honeycomb-like pattern. Due to the having extraordinary properties such as lightness and strength, graphene can be abundantly applied in engineering structures such as aerospace structure (Kuzhir *et al*. 2013), bio-structures (Ali *et al*. 2017). On the other hand, Graphene sheets (GSs) are the two dimensional structures containing unbeatable lattice structures, supreme electronic and mechanical characteristics. So far, a number of techniques have been extended to attain GSs including Hummer method and exfoliation (Marina *et al*. 2016 and Ali *et al*. 2015), exfoliation of graphite in solvents, micromechanical exfoliation (Al-Sherbini *et al*. 2017, Tasis *et al*. 2013, Siddique *et al*. 2015). Until today, many investigation projects have been conducted to investigate the mechanical behaviors of the single-layered graphene sheet (SLGS) such as free and forced vibration (Sakhaee-Pour *et al*. 2008, Song *et al*. 2017), buckling (Sakhaee-Pour 2009, Rouhi and Ansari 2012), and bending (Sobhy 2014 and Wei *et al*. 2012) behaviors. A hybrid atomistic-structural element proposed by Sadeghi and Naghdabadi (2010) to investigate the infinitesimal and large amplitude of SLGS.

Today, a life without nanotechnology is hard to imagine. Utilizing nanotechnology, materials can effectively be made stronger, lighter, more durable, more reactive, more sieve-like, or better electrical conductors, among many other traits.

Considering the importance of investigating the behavior of nanostructures, some researchers utilized empirical testing and atomistic simulation results (Chen *et al*. 2006, Stan *et al*. 2007) to demonstrate this theorem that by reducing the material size to the micro/neon scale, the effect of size-dependent materials becomes remarkable. Formerly, the weakness of the classical continuum theories to capture the size effect has been proved by researchers. Hence, certain higher-order continuum theories containing the independent internal length scale parameter have been developed (Eringen 1983, Lam *et al*. 2003, Yang *et al*. 2002, Lim *et al*. 2015). One of these non-traditional theories is called nonlocal elasticity theory proposed by Eringen (1983) including a material length scale term to predict the size effect. Because of modelling carbon nanotubes and fullerenes as GSs in applications, studying the behavior of GSs in micro/nano scale is a significant subject. By taking into account nonlocal elasticity theory in conjunction with the first-order shear deformation theory (FSDT), Ansari *et al*. (2010) investigated the resonant frequencies of SLGS under various boundary conditions using generalized differential quadrature method (GDQM). The authors employed the molecular dynamics (MD) approach for

*Corresponding author, Ph.D. Student,
E-mail: vahid.th1982@gmail.com; vahid.tahouneh@ut.ac.ir

ISSN: 1229-9367 (Print), 1598-6233 (Online)

estimating the suitable values of nonlocal parameter. Pradhan and Kumar (2010) studied the natural frequencies of orthotropic SLGS via nonlocal differential constitutive relations of Eringen (1983). Applying the kp-Ritz method with the nonlocal continuum assumption, Zhang *et al*. (2015) analyzed the free vibration of SLGS. Based on the nonlinear von Kármán terms and nonlocal elasticity theory, Ribeiro and Chuaqui (2019) examined the nonlinear modes of vibration of SLGS using Airy stress function. Kumar and Srivastava (2016) studied Elastic properties of CNT- and Graphene-reinforced nanocomposites using RVE. Hosseini and Zhang (2018) considered transient dynamic analysis and elastic wave propagation in a functionally graded graphene platelets (FGGPLs)-reinforced composite thick hollow cylinder, which is subjected to shock loading. Soleimani *et al*. (2019) investigated the effects of inevitable out-of-plane defects on the postbuckling behavior of single-layered graphene sheets (SLGSs) under in-plane loadings based on nonlocal first order shear deformation theory. Moradi-Dastjerdi and Behdinan (2019) studied thermoelastic static and free vibrational behaviors of axisymmetric thick cylinders reinforced with functionally graded (FG) randomly oriented graphene subjected to internal pressure and thermal gradient loads. Javani *et al*. (2019) studied buckling analyses of composite plate reinforced by Graphen platelate (GPL). Karami *et al*. (2018b) used three-dimensional (3D) elasticity theory in conjunction with nonlocal strain gradient theory (NSGT) to develop for mechanical analysis of anisotropic nanoparticles. Ahmed Houari *et al*. (2018) presented ~~a~~ closed-form solutions for exact critical buckling loads of nonlocal strain gradient functionally graded beams. Shahsavari *et al*. (2018) developed a high-order nonlocal strain gradient model for wave propagation analysis of porous FG nanoplates resting on a gradient hybrid foundation in thermal environment. Convective heat transfer performance and fluid flow characteristics of Cu-Ag/water hybrid nanofluids investigated by Hassan *et al*. (2018). Othman and Marin (2017) studied the wave propagation of generalized thermoelastic porous medium under the effect of thermal loading due to laser pulse with energy dissipation. Karami *et al*. (2017) investigated the influences of triaxial magnetic field on the wave propagation behavior of anisotropic nanoplates. Karami *et al*. (2018a) used a new size-dependent quasi-3D plate theory for wave dispersion analysis of functionally graded nanoplates while resting on an elastic foundation and under the hygrothermal environment. Marin (1999) used the theory of semigroups of operators in order to obtain the existence and uniqueness of solutions for the mixed initial-boundary value problems in thermoelasticity of dipolar bodies. Marin and Craciun (2017) considered aboundary value problem in dipolar thermoelasticity to model composite materials to obtain uniqueness results. Marin (1994) developed the Lagrange identity method for the study of the initial boundary value problem of thermoelasticity of bodies with microstructure. Tornabene *et al*. (2018) studied free vibration of laminated nanocomposite plates and shells using first-order shear deformation theory and the Generalized Differential Quadrature (GDQ) method. Each layer of the laminate was modelled as a three-phase composite. A survey of several methods under the heading of strong formulation finite element method (SFEM) was presented by Tornabene *et al*. (2015). These approaches were distinguished from classical one, termed weak formulation finite element method (WFEM). Isogeometric approach, an efficient and useful numerical method, has been introduced by Hughes *et al*. (2005) which fulfills a gap between computer aided design (CAD) and finite element analysis (FEA). Main ideas of this method are to adopt the CAD basis functions (e.g., the NURBS) to the shape functions in the finite element analysis. Bilotta *et al*. (2010) proposed a three-dimensional finite element, named HC3, based on a quadratic B-spline interpolation of the displacement field for the linear elastic analysis of three-dimensional problems. This proposed element was an extension of the high-continuity (HC) finite element presented by Aristodemo (1985) for two-dimensional elasticity which is the first investigation on the HC finite element. The accuracy and efficiency of the isogeometric analysis for structures such as beams and plates have been demonstrated by a number of works in these years, e.g. (Guo *et al*. 2014, Kapoor and Kapania 2012, Le-Manh and Lee 2014, Le-Manh *et al*. 2016, Malagu *et al*. 2012, Thai *et al*. 2012, Tran *et al*. 2015, 2016, Wang *et al*. 2015, Yu *et al*. 2015). Soleimani *et al*. (2017) investigated the critical buckling loads of GSs under various values of nonlocal parameters and different boundary conditions using IGA based on NURBS. Also, IGA is taken into account to analyze the thermal buckling problem of composite laminated plates reinforced with GSs by Mirzaei and Kiani (2017). Due to the fact that during the production process and under constrains conditions, it is possible SLGS may be defected (Compagnini *et al*. 2009, Martinez-Asencio and Caturla 2015, Sun *et al*. 2013 and Rajasekaran *et al*. 2016), therefore, it is critical to study the influence of these structural defects such as vacancies on the mechanical characteristics of SLGS. On the other hand, cut-outs or vacancies may be made to lighten the structure or to alter the resonant frequencies of SLGS. According to the nonlocal continuum assumption, the effect of defect modeled as eccentric hole on the elastic instability of an annular SLGS resting on elastic medium is analytically reported by Fadaee (2016) applying translational addition theorem. Dastjerdi *et al*. (2016) developed a nonlocal model based upon FSDT to analyze the bending problem of annular SLGS under with an eccentric vacant defect. The authors demonstrated that the influence of attendance of vacancy defect extremely depends on the kinds of boundary conditions. Mirakhory *et al*. (2018) obtained the natural frequencies of the defected triangular GSs and reported that the defective equilateral triangular GSs have the highest values of resonance. Employing the Monte Carlo simulation based finite element method, Chu *et al*. (2018) investigated the natural frequencies of vacancy defected GSs. They indicated that an increase in the value of thickness and Young's modulus of GSs leads to smaller values of natural frequencies. The preceding review explicitly denoted that there is an increasing amount of investigations on the mechanical behavior of SLGS via nonclassical continuum theories. However, there seems to be no systematic, analytical or numerical studies on utilizing the Kirchhoff plate assumption in conjunction with nonlocal elasticity theory to investigate the free vibration of SLGS with a cut out via IGA based upon NURBS using trimming technique. Thus, the main aim of current work is to fill this major gap in the present literature. During the numerical analysis, the natural frequency of the defected SLGS is calculated and compared with those of previous researches.

2. Isogeometric formulation for vibration analysis

2.1 NURBS basis functions

A brief fundamental of some technical features of B-spline and NURBS basis functions for isogeometric analysis is presented. A detailed description of the NURBS, one may reach, e.g., see Piegl and Tiller (1997). A NURBS curve $\mathbf{X}(\xi)$ of order p is defined as

$$X(\xi)=\sum_{i=1}^{n}R_{i,p}(\xi)\tilde{X}_i, \tag{1}$$

$$R_{i,p}(\xi)=\frac{N_{i,p}(\xi)\omega_i}{\sum_{j=1}^{n}N_{j,p}(\xi)\omega_j}, \tag{2}$$

where $R_{i,p}$ stands for the univariate NURBS basis functions, $\tilde{X}_i=(x_i, y_i)$; $i = 1, 2, ..., n$ are a set of n control points, wi are a set of n weights corresponding to the control points that must be non-negative and $N_{i,p}$ represents the B-spline basis function of order p. To construct a set of n B-spline basis functions of order p, a knot vector Ξ is defined in a parametric space as

$$\Xi=\{\xi_1,\xi_2,...,\xi_{n+p+1}\}\quad \xi_i\le\xi_{i+1},\quad i=1,2,...,n+p \tag{3}$$

The parametric space is assumed to be $\xi\in[0, 1]$. The knot vectors used for analysis purposes are generally open knot vectors to satisfy the Kronecker-delta property at boundary points (Roh and Cho 2004). The knot vector is said to be open if the knots are repeated p+1 times at the start and end of the vector. Given a knot vector, the univariate B-spline basis function $N_{i,p}$ can be constructed by the following Cox-de Boor recursion formula (Piegl and Tiller 1997)

$$N_{i,0}(\xi)=\begin{cases}1 \quad \text{if} \quad \xi_i\le\xi\le\xi_{i+1}\\ 0 \quad\quad \text{otherwise}\end{cases} \tag{4}$$

and

$$\begin{aligned}N_{i,p}(\xi)&=\frac{\xi-\xi_i}{\xi_{i+p}-\xi_i}N_{i,p-1}(\xi)\\&+\frac{\xi_{i+p+1}-\xi}{\xi_{i+p+1}-\xi_{i+1}}N_{i+1,p-1}(\xi),\\ p&=1,2,3,...\end{aligned} \tag{5}$$

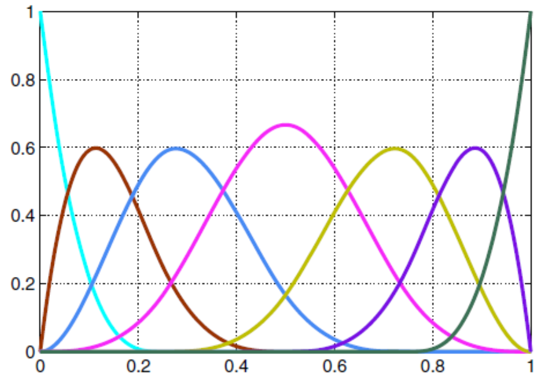

Fig. 1 Cubic basis functions for an open knot vector Ξ = {0,0,0,0,0.25,0.5,0.75,1,1,1,1}

The B-spline functions which are constructed from the open knot vectors have the interpolation feature at the ends of the parametric space. A cubic B-spline basis functions with the interpolation feature at the ends of the parametric space are shown in Fig. 1. Generally, a NURBS surface of order p in ξ direction and order q in η direction can be expressed as

$$\begin{aligned}X(\xi,\eta)&=\sum_{i=1}^{n}\sum_{j=1}^{m}R_{i,j}^{p,q}(\xi,\eta)\tilde{X}_{i,j}\\&=\sum_{i=1}^{n}\sum_{j=1}^{m}\frac{N_{i,p}(\xi)M_{j,q}(\eta)\omega_{i,j}}{\sum_{\hat{i}}^{n}\sum_{\hat{j}}^{m}N_{\hat{i},p}(\xi)M_{\hat{j},q}(\eta)\omega_{\hat{i},\hat{j}}}\tilde{X}_{i,j}\\&0\le\xi,\eta\le1\end{aligned} \tag{6}$$

where $R_{i,j}^{p,q}$ stands for the bivariate NURBS basis functions, $\tilde{X}_{i,j}$ is a control mesh of n×m control points, and $\omega_{i,j}$ are the corresponding weights, while $N_{i,p}$ and $M_{j,q}$ are the B-spline basis functions defined on the Ξ and H knot vectors, respectively. The first derivative of $R_{i,j}^{p,q}(\xi,\eta)$ with respect to each parametric variable, e.g., ξ, is derived by simply applying the quotient rule to Eq. (6) as

$$\frac{\partial R_{i,j}^{p,q}(\xi,\eta)}{\partial\xi}=\frac{\frac{\partial N_{i,p}(\xi)}{\partial\xi}M_{j,q}(\eta)\omega_{i,j}W(\xi,\eta)-\frac{\partial W(\xi,\eta)}{\partial\xi}N_{i,p}(\xi)M_{j,q}(\eta)\omega_{i,j}}{(W(\xi,\eta))^2} \tag{7}$$

and

$$W(\xi,\eta)=\sum_{\hat{i}}^{n}\sum_{\hat{j}}^{m}N_{\hat{i},p}(\xi)\,M_{\hat{j},q}(\eta)\omega_{\hat{i},\hat{j}} \tag{8}$$

$$\frac{\partial W(\xi,\eta)}{\partial\xi}=\sum_{\hat{i}}^{n}\sum_{\hat{j}}^{m}\frac{\partial N_{\hat{i},p}(\xi)}{\partial\xi}M_{\hat{j},q}(\eta)\omega_{\hat{i},\hat{j}} \tag{9}$$

To earn more detail about the NURBS and its characteristics, the reader is referred to Ref. (Piegl and Tiller 1997). It is worthwhile to note that in the IGA analysis, by using the isoparametric concept, the NURBS basis is employed for both the parametrization of the

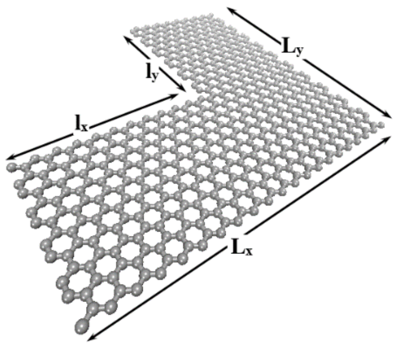

Fig. 2 The Schematic of a SLGS with corner cutout

geometry and the approximation of the solution field, which is the plate deflection w(x) in this paper, as follows

$$w^h(x(\xi)) = \sum_{I=1}^{n\times m} \phi_I(\xi) w_I \tag{10}$$

$$x(\xi) = \sum_{I=1}^{n\times m} \phi_I(\xi) \tilde{x}_I \tag{11}$$

In all the above equations, ξ = (ξ, η) is the parametric coordinates, **x** = (*x*,*y*) is the physical coordinates, $\tilde{x}_I$ represents the control points of a n×m control mesh, w_I represents the deflection of the plate at each control point, and $\phi_I(\xi)$ are the bivariate NURBS functions of order p and q in ξ and η directions, respectively.

2.2 Governing equations for a L-shape SLGS

As schematically illustrated in Fig. 2, a SLGS (uniform thickness *h*, length L_x and width L_y) with corner rectangular cutout (l_x*l_y) is considered along with the cartesian coordinate system. The L-shape plate is assumed to be Free (F) in the straight edges of cutout while any arbitrary boundary conditions are applied to the other four straight edges including Simply supported (S), Clamped (C) and Free (F). Furthermore, the transverse displacement of the defected SLGS is expressed with w.

Employing the classical laminated plate (Kirchhoff) assumption, the displacement parts $(u_x,\ u_y,\ u_z)$ for an optional point can be presented as (Liu 2003)

$$\begin{aligned} &u_x = -z\frac{\partial w(x,y,t)}{\partial x}, \qquad u_y = -z\frac{\partial w(x,y,t)}{\partial y}, \\ &u_z = w(x,y,t) \\ &\{u_x, u_y, u_z\} = \left\{-z\frac{\partial}{\partial x} \quad -z\frac{\partial}{\partial y} \quad 1\right\}^T w = Tw \end{aligned} \tag{12}$$

Utilizing Eq. (12), the linear strain components are denoted as

$$\begin{aligned} &\varepsilon_{xx} = -z\frac{\partial^2 w}{\partial x^2}\ ,\ \varepsilon_{yy} = -z\frac{\partial^2 w}{\partial y^2}\ ,\gamma_{xy} = -2z\frac{\partial^2 w}{\partial x \partial y} \\ &\{\varepsilon_{xx}, \varepsilon_{yy}, \gamma_{xy}\} = z\left\{-\frac{\partial^2}{\partial x^2} \quad -\frac{\partial^2}{\partial y^2} \quad -2\frac{\partial^2}{\partial x \partial y}\right\}^T w = Lw \end{aligned} \tag{13}$$

In which ε_{xx} and ε_{yy} demonstrate the normal strain members, and the term γ_{xy} denotes the shear strain part. By taking into account the plane stress assumption and using the nonlocal constitutive equation of Eringen (1983), the nonlocal constitutive stress-strain relations for an orthotropic SLGS can be expressed as below

$$\begin{aligned} &(1-\mu\nabla^2)\begin{Bmatrix} \sigma_{xx}^{nl} \\ \sigma_{yy}^{nl} \\ \sigma_{xy}^{nl} \end{Bmatrix} \\ &= \begin{bmatrix} \frac{E_1}{(1-\upsilon_{12}\upsilon_{21})} & \frac{\upsilon_{12}E_2}{(1-\upsilon_{12}\upsilon_{21})} & 0 \\ \frac{\upsilon_{12}E_2}{(1-\upsilon_{12}\upsilon_{21})} & \frac{E_2}{(1-\upsilon_{12}\upsilon_{21})} & 0 \\ 0 & 0 & G_{12} \end{bmatrix} \begin{Bmatrix} \varepsilon_{xx} \\ \varepsilon_{yy} \\ \gamma_{xy} \end{Bmatrix} \end{aligned} \tag{14}$$

Where E_1 and E_2 are, respectively, the Young's moduli in orientations 1 and 2. Also, G_{12} refers to the shear modulus, and Poisson's ratios are presented with ϑ_{12} and ϑ_{21} . Furthermore, the symbol $\mu = (e_0 a)^2$ is the nonlocal term, which is able to consider the small scale effect into the governing equations of the motion. However, e_0 refers to the calibration coefficients, which can be determined from experiment or the results of MD simulation. It should be noted that here, a is the internal characteristic length and $\nabla^2 = \frac{\partial^2}{\partial x^2} + \frac{\partial^2}{\partial y^2}$ demonstrates the two-dimensional Laplacian operator. Applying the linear strain components of Eq. (13) and the nonlocal constitutive stress-strain relations of Eq. (14), the stress resultants in terms of transverse deflection of an orthotropic SLGS can be written as (Hosseini Hashemi *et al*. 2015)

$$\begin{aligned} &M_{xx}(1-\mu\nabla^2) = -D_{11}\frac{\partial^2 w}{\partial x^2} - D_{12}\frac{\partial^2 w}{\partial y^2}, \\ &M_{yy}(1-\mu\nabla^2) = -D_{22}\frac{\partial^2 w}{\partial y^2} - D_{12}\frac{\partial^2 w}{\partial x^2}, \\ &M_{xy}(1-\mu\nabla^2) = -2D_{66}\frac{\partial^2 w}{\partial x \partial y} \end{aligned} \tag{15}$$

where

$$(M_{xx}, M_{yy}, M_{xy}) = \int_{-\frac{\square}{2}}^{\frac{\square}{2}} (\sigma_{xx}^{nl}, \sigma_{yy}^{nl}, \sigma_{xy}^{nl}) z dz \tag{16}$$

$$\begin{aligned} &D_{11} = \frac{E_1 h^3}{12(1-\upsilon_{21}\upsilon_{12})}, \quad D_{12} = \frac{\upsilon_{12}E_2 h^3}{12(1-\upsilon_{21}\upsilon_{12})} \\ &D_{22} = \frac{E_2 h^3}{12(1-\upsilon_{21}\upsilon_{12})}, \quad D_{66} = \frac{G_{12}h^3}{12} \end{aligned} \tag{17}$$

It is noteworthy that for free vibration problem, the matrix-vector expressions of the strain energy Π_U and kinetic energy Π_T can be defined as

$$\Pi_U = \frac{1}{2}\int_V \varepsilon^T \sigma dV, \quad \Pi_T = \frac{1}{2}\int_V \rho \dot{u}^T \dot{u} dV \tag{18}$$

Where V stands for the volume of orthotropic SLGS. Now, Hamilton's variational principle is used to achieve the governing differential equations of motion equation (Norouzzadeh and Ansari 2018)

$$\delta\int_{t_1}^{t_2}(\Pi_T-\Pi_U)dt=0 \tag{19}$$

By substituting the deflection w from Eq. (10), the final undamped dynamic discrete equations for free vibration analysis in the present isogeometric method can be derived as

$$M\ddot{w}+Kw=0 \tag{20}$$

where w and $\ddot{w}$ are the vectors of the deflection and acceleration at the control points. K and M, respectively, stand for global stiffness and mass matrices which are defined as

$$K_{IJ}=\int_A B_I^T\,DB_J dA \tag{21}$$

$$M_{IJ}=\int_A\left\{\begin{matrix}(\frac{\rho h^3}{12})(\frac{\partial\phi_I}{\partial x}\frac{\partial\phi_J}{\partial x}+\frac{\partial\phi_I}{\partial y}\frac{\partial\phi_J}{\partial y})+\\ \rho h\phi_I(1-\mu\nabla^2)\phi_J\end{matrix}\right\}dA \tag{22}$$

$$B_I=\left\{-\frac{\partial^2\phi_I}{\partial x^2}\quad-\frac{\partial^2\phi_I}{\partial y^2}\quad-2\frac{\partial^2\phi_I}{\partial x\partial y}\right\}^T \tag{23}$$

In the above-mengtioned equations, ρ and h are the density and thickness of the plate, respectively. A general solution for the homogenous equation given in Eq. (20) can be written as

$$w=\bar{w}e^{i\omega t} \tag{24}$$

Here i is the imaginary unit, ω indicates natural frequency, t represents time, and $\bar{w}$ is the eigenvector. By substituting Eq. (24) into Eq. (20), the natural frequency ω of the free vibration of the plate can be obtained by solving the following eigenvalue equation

$$(K-\omega^2M)\bar{w}=0 \tag{25}$$

2.3 Boundary conditions and trimming technique

In this paper, we use a simple and efficient technique which was first proposed by Kiendl *et al*. (2009) for analysis of shell structures. In this technique, clamped boundary conditions can be imposed by simply fixing the deflection of the plate at the first two rows of control points from the desired boundary. This is based on the fact that the slopes at the boundary of a NURBS surface are defined by the first two rows of control points from this boundary (Kiendl *et al*. 2009). Simply supported boundary condition is also imposed by fixing the deflection of the first row of control points from the boundary.

In this study, the trimming technique is used to make rectangular corner cut out in a graphene. In this method, the

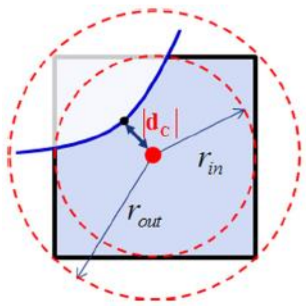

Fig. 3 Searching for closest point from the center point of each element to trimming path (Kim *et al*. 2010)

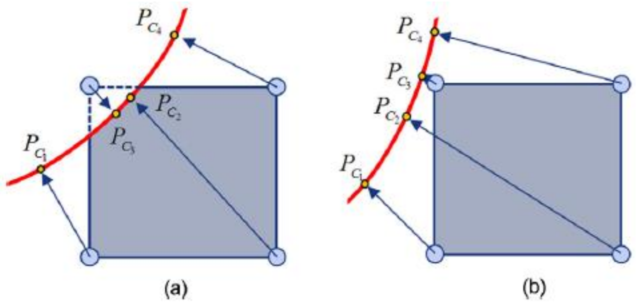

Fig. 4 Next stage to make clear the trimmed elements: (a) trimmed element; and (b) non-trimmed element (Kim *et al*. 2010)

closest point from the center of each element to the trimming curve is searched as shown in Fig. 3. If the distance (d_c) from the center point to the closest point is less than the radius of the inscribed circle (r_{in}), it is a trimmed element. If the d_c is greater than the radius of circumscribed circle (r_{out}), it is a non-trimmed element. For the case $r_{in}\leq d_c<r_{out}$ further searching step is required. For the second step, discrimination scheme of the four vertex points of the element is performed. Then four closest points $(P_{C1}-P_{C4})$ can be found as shown in Fig. 4. If at least one closest point is located inside the element, the element is a trimmed one (Fig. 4(a)). Otherwise it is a non-trimmed element (Fig. 4(b)). Note that the shape of element in parametric domain is always rectangular or square. It should be noted that because of considering the straight edges trimming for making the corner cutout in this study, the procedure could be simpler than those above mentioned approaches. However, using this searching algorithm trimmed elements in any complicated situations can be successfully searched. To earn more detailed information about how to find trimmed elements, the reader is referred to Ref. (Kim *et al*. 2010).

3. Numerical simulations

3.1 Validation and comparison study

To show the correctness and validity of the achieved formulation, several numerical examples with different boundary conditions are investigated in this section. The

Table 1 Comparison study of the non-dimensional natural frequencies of completely free isotropic square plate

Mode	Present method (12*12)	Liu and Chen (2001)	Analytical solution (Abbassian *et al*. 1987)	FEM (Abbassian *et al*. 1987)	
				HOE	LOE
4	3.670	3.670	3.670	3.567	3.682
5	4.427	4.429	4.427	4.423	4.466
6	4.927	4.930	4.926	4.875	4.997
7	5.900	5.901	5.929	5.851	5.942
8	5.900	5.901	5.929	5.851	5.942
9	7.818	7.832	7.848	7.820	8.079

Table 2 Comparison study of the non-dimensional natural frequencies of simply supported isotropic square plate

Mode	Present method (12*12)	Analytical solution (Abbassian *et al*. 1987)	Liu and Chen (2001)	
			Regular nodes	Irregular nodes
1	4.443	4.443	4.443	4.453
2	7.025	7.025	7.031	7.033
3	7.025	7.025	7.036	7.120
4	8.886	8.886	8.892	8.912
5	9.938	9.935	9.959	9.966
6	9.938	9.935	9.966	10.010
7	11.329	11.327	11.341	11.345
8	11.329	11.327	11.341	11.540
9	12.971	-	13.032	12.994
10	12.971	-	13.036	13.064

Table 3 Comparison study of the non-dimensional natural frequencies of fully clamped isotropic square plate

Mode	Present method (12*12)	Analytical solution (Abbassian *et al*. 1987)	Liu and Chen (2001)	
			Regular nodes	Irregular nodes
1	5.999	5.999	6.017	5.999
2	8.568	8.568	8.606	8.596
3	8.568	8.568	8.606	8.602
4	10.401	10.407	10.439	10.421
5	11.469	11.472	11.533	11.507
6	11.496	11.498	11.562	11.528
7	12.829	-	12.893	12.925
8	12.829	-	12.896	12.986
9	14.468	-	14.605	14.570
10	14.468	-	14.606	14.604

obtained results of present isogeometric approach are verified by comparing with other numerical or analytical solutions available in the literature. Firstly, Natural frequencies of an isotropic square plate without considering nonlocal term, and three types of boundary condition including Free (F), Simply supported (S) and Clamped (C) are investigated. The natural frequencies of a free square plate are listed in Table 1. It is observed that the calculated results are in good agreement with the results of other research works. In this table, HOE denotes eight-nodes semi-loof thin shell element (4*4 mesh); LOE denotes four-noded iso-parametric shell element (8*8 mesh). The first three frequencies corresponding to the rigid displacements are zero and are not reported. Natural frequencies of a simply supported and fully clamped square plates are computed using the present method. The results are shown in Tables 2 and 3, from these tables, one can find that present results are in good agreement with those of the other solutions.

To testify the validity of the present method, a comparison between the fundamental natural frequency obtained for an isotropic square nanoplate against different values of the nonlocal parameters with those obtained by other researchers (Norouzzadeh and Ansari 2018, Nguyen *et al*. 2015, Aghababaei and Reddy 2009) is indicated in Table 4. By briefly reviewing the computed results in this table, the accuracy of present formulations is determined.

As another example to assess accuracy and reliability of present work, natural frequencies of completely free and simply supported isotropic L-shape plate are calculated and listed in Tables 5 and 6. An appropriate conformity is seen with the IGA results in present study and those of obtained by other researchers (Bui and Nguyen 2011). All above-mentioned results demonstrate that the present method is suitable and efficient in performing free vibration analysis of plates with different shapes including rectangular and L-shape ones.

3.2 Benchmark results of a graphene sheet with corner cutout

Numerical computations are carried out in this section to better understand the impact of various parameters (nonlocal parameter, cutout dimensions, mode number and boundary condition) on the variation of the system natural frequency. In this study we consider a graphene sheet with a size of $L_x = L_y = 10$ *nm*. The mechanical properties of SLGSs are taken from (Kitipornchai *et al*. 2005) as:

Young's modulus E = 1.06 *TPa*, Poisson's ratio $\boldsymbol{\upsilon}$ = 0.16, density ρ = 2250 kg/m^3 and effective thickness h = 0.34 *nm*. According to the results reported in section 3, considering 144 control points can lead to good results and convergence so other results are further calculated with this number of control points.

In this stage, the non-dimensional natural frequency is defined as follows

$$\Omega = \left(\frac{\omega^2 L_x^4 \rho h}{D}\right)^{\frac{1}{4}}, \quad D = \frac{Eh^3}{12(1-\upsilon^2)} \tag{26}$$

Table 4 Non-dimensional natural frequency of fully simply supported isotropic square nanoplate

a/h	μ (nm^2)	Present method	Norouzzadeh and Ansari (2018)	Nguyen *et al* (2015)		Aghababaei and Reddy (2009)		
				RPT	Quasi-3D	TSDT	FSDT	CPT
10	0	0.0955	0.0931	0.0930	0.0920	0.0935	0.0930	0.0963
	1	0.0874	0.0850	0.0850	0.0841	0.0854	0.0850	0.0880
	2	0.0811	0.0788	0.0788	0.0779	0.0791	0.0788	0.0816
	3	0.0759	0.0738	0.0737	0.0729	0.0741	0.0737	0.0763
	4	0.0717	0.0696	0.0695	0.0688	0.0699	0.0696	0.0720
20	0	0.0240	0.0239	0.0239	0.0239	0.0239	0.0239	0.0241
	1	0.0219	0.0218	0.0218	0.0218	0.0218	0.0218	0.0220
	2	0.0203	0.0202	0.0202	0.0202	0.0202	0.0202	0.0204
	3	0.0190	0.0189	0.0189	0.0189	0.0189	0.0189	0.0191
	4	0.0179	0.0178	0.0178	0.0178	0.0179	0.0178	0.0180

Table 5 Non-dimensional natural frequency of completely free isotropic L-shape plate. The first three frequencies corresponding to rigid displacements are not listed

Mode	Present method (12*12)	MKI (Bui and Nguyen 2011)	EFG (Bui and Nguyen 2011)
4	4.0971	3.9694	3.9796
5	4.1336	4.1284	4.1790
6	5.5736	5.2122	5.2253
7	5.8228	5.7109	5.8294
8	7.7262	7.6153	7.7726
9	7.9601	7.7838	7.8009
10	8.4220	8.1233	8.0450

Table 6 Non-dimensional natural frequency of simply supported isotropic L-shape plate

Mode	Present method (12*12)	MKI (Bui and Nguyen 2011)	EFG (Bui and Nguyen 2011)
4	6.9070	6.8204	6.7649
5	8.0100	7.9560	8.0319
6	8.8989	8.4489	8.8821
7	10.7011	10.4509	10.8853
8	11.6223	11.1064	11.5584
9	13.7435	13.2219	13.0156
10	13.7695	13.3820	13.7309

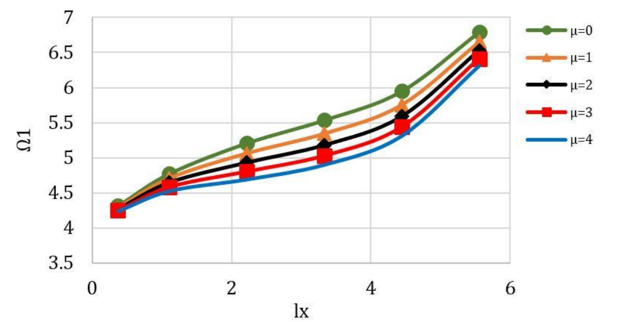

Fig. 5 The effect of cutout dimensions (l_x) on the first dimensionless natural frequency of CCCCFF L-shape SLGS

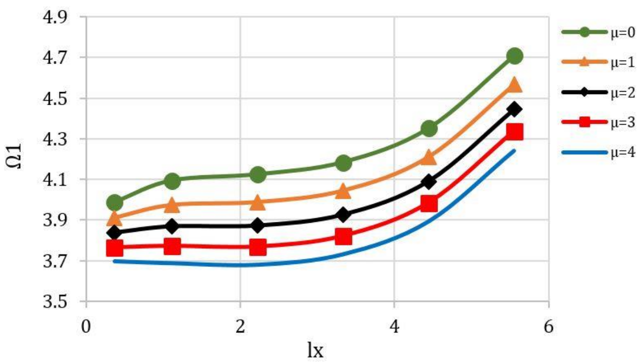

Fig. 6 The effect of cutout dimensions (l_x) on the first dimensionless natural frequency of SSSSFF L-shape SLGS

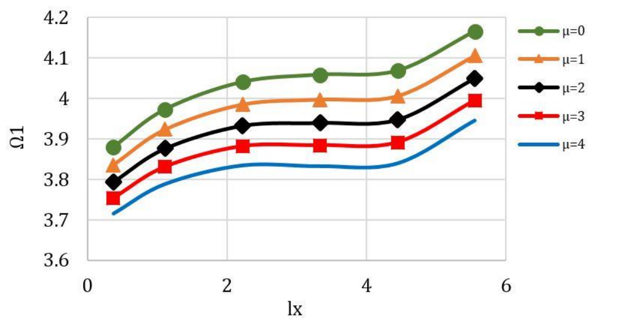

Fig. 7 The effect of cutout dimensions (l_x) on the first dimensionless natural frequency of FFFFFF L-shape SLGS

The effects of increasing size of cutout on the first natural frequency is investigated in Figs. 5, 6 and 7.

Figs. 5, 6 and 7 show results for CCCCFF, SSSSFF and FFFFFF edge conditions, respectively. Results are plotted for a graphene with square cutout size of 0.37 *nm*, 1.11 *nm*, 2.22 *nm*, 3.33 *nm*, 4.44 *nm*, 5.55 *nm* and various nonlocal parameters. These figures show that an increasing the size of cutout will lead to increase the natural frequency of structure. Also, Because of the softening effect of nonlocal term on the system, the natural frequency decreases by increasing nonlocal parameter. But in lower cutout's size, the effect of the nonlocal parameters scaled down.

The influence of the nonlocal parameter on natural frequencies of CCCCFF, SSSSFF and FFFFFF L-shape plate is depicted in Figs. 8, 9 and 10, respectively. Results are presented for three mode numbers and the square cutout size of 1.11 *nm*. It is observed that an increasing nonlocal parameter decreases the natural frequencies for each mode number. It is also seen that decreasing nonlocal parameter has more effects on higher modes with respect to lower ones.

To make clear the effect of boundary condition on the natural frequencies of L-shape plate, the third mode frequencies of L-shape SLGS with CCCCFF, SSSSFF and FFFFFF boundary conditions are compared in Fig. 11. The natural frequency of CCCCFF L-shape GS is significantly higher than those of L-shape GS with SSSSFF and FFFFFF boundary conditions.

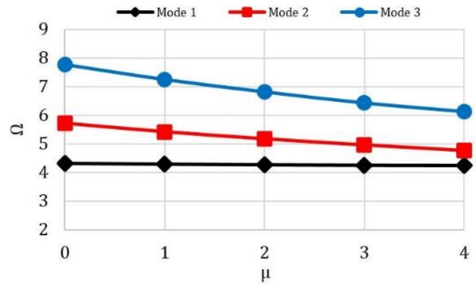

Fig. 8 The effect of nonlocal parameter on the dimensionless natural frequencies of CCCCFF L-shape SLGS for different mode numbers

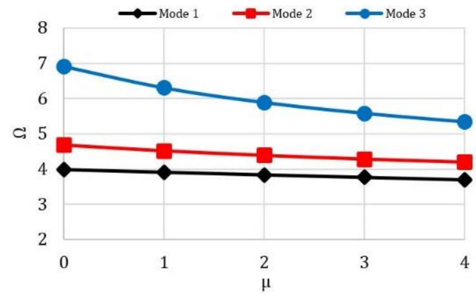

Fig. 9 The effect of nonlocal parameter on the dimensionless natural frequencies of SSSSFF L-shape SLGS for different mode numbers

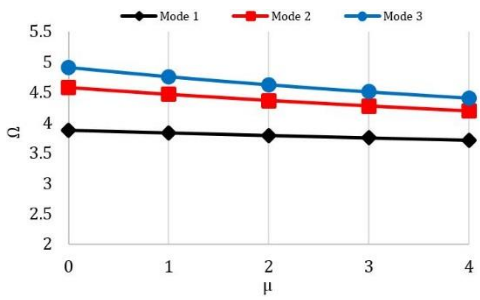

Fig. 10 The effect of nonlocal parameter on the dimensionless natural frequencies of FFFFFF L-shape SLGS for different mode numbers

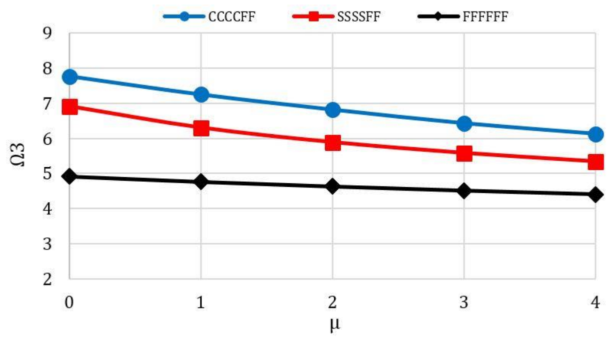

Fig. 11 The influence of nonlocal parameter and different type of boundary conditions on the third mode frequency of L-shape SLGS

As expected, increasing the degrees of freedom in the edges, decreases the natural frequencies. It is worth noting that this effect has been seen in other mode numbers but for the sake of brevity, they are not reported here.

4. Conclusions

A NURBS based on IGA is exhibited to analyze the behavior of free vibration of a SLGS with corner cutout via nonlocal elasticity approach utilizing the Kirchhoff plate assumption. Trimming technique, very fast and accurate procedure for analysis of complicated geometries, with a single patch is employed to create the cutout in geometry of L-shape plate. The L-shape plate is assumed to be Free (F) in the straight edges of cutout while any arbitrary boundary conditions are applied to the other four straight edges including Simply supported (S), Clamped (C) and Free (F). The correctness of the obtained results is checked via comparing with existing data in the literature and good agreement is eventuated. As a result, the effectiveness and the accuracy of the present IGA approach have been demonstrated and it is shown that the IGA is efficient, robust and accurate in terms of nanoplate problems. From this study some conclusions can be made as following:

- It is shown that the classical continuum model tends to overestimate the natural frequencies of a GS, and the nonlocal theory must be applied to reduce the relative error.
- It is observed that an increasing nonlocal parameter decreases the natural frequencies for each mode number.
- It is also seen that decreasing nonlocal parameter has more effects on higher modes with respect to lower ones.
- Results reveal that in lower cutout's size, the effect of the nonlocal parameters scaled down.
- It is seen that an increasing the size of cutout will lead to increase the natural frequency of structure.

This study serves as a benchmark for assessing the validity of numerical methods used to analyze the single-layered graphene sheet with corner cutout.

References

Abbassian, F., Dawswell, D.J. and Knowles, N.C. (1987), "Free Vibration Benchmarks. Atkins Engineering Sciences", Glasgow.

Aghababaei, R. and Reddy, J.N. (2009), "Nonlocal third-order shear deformation plate theory with application to bending and vibration of plates", *J. Sound Vib.*, **326**(1-2), 277-289. https://doi.org/10.1016/j.jsv.2009.04.044

Ahmed Houari, M.S., Bessaim, A., Bernard, F., Tounsi, A. and Mahmoud, S.R. (2018), "Buckling analysis of new quasi-3D FG nanobeams based on nonlocal strain gradient elasticity theory and variable length scale parameter", *Steel Compos. Struct., Int. J.*, **28**(1), 13-24. https://doi.org/10.12989/scs.2018.28.1.013

Al-Sherbini, A.S., Bakr, M., Ghoneim, I. and Saad, M. (2017), "Exfoliation of graphene sheets via high energy wet milling of graphite in 2-ethylhexanol and kerosene", *J. Adv. Res.*, **8**(3), 209-215. https://doi.org/10.1016/j.jare.2017.01.004

Ali, G.A.M., Makhlouf, S.A., Yusoff, M.M. and Chong, K.F. (2015), "Structural and electrochemical characteristics of graphene nanosheets as supercapacitor electrodes", *Rev. Adv. Mater. Sci.*, **41**(1), 35-43.

Ali, M.A., Mondal, K., Wang, Y., Jiang, H., Mahal, N.K., Castellano, M.J., Sharma, A. and Dong, L. (2017), "*In situ* integration of graphene foam-titanium nitride based bio-scaffolds and microfluidic structures for soil nutrient sensors", *Lab. Chip.*, **17**(2), 274-285. https://doi.org/10.1039/C6LC01266C

Ansari, R., Sahmani, S. and Arash, B. (2010), "Nonlocal plate model for free vibrations of single-layered graphene sheets", *Phys. Lett. A.*, **375**(1), 53-62. https://doi.org/10.1016/j.physleta.2010.10.028

Aristodemo, M. (1985), "A high-continuity finite element model for two dimensional elastic problems", *Comput. Struct.*, **21**(5), 987-993. https://doi.org/10.1016/0045-7949(85)90211-1

Bilotta, A., Formica, G. and Turco, E. (2010), "Performance of a high-continuity finite element in three-dimensional elasticity", *Int. J. Numer. Methods Biomed. Eng.*, **26**(9), 1155-1175. https://doi.org/10.1002/cnm.1201

Bui, T.Q. and Nguyen, M.N. (2011), "A moving Kriging interpolation-based meshfree method for free vibration analysis of Kirchhoff plates", *Comput. Struct.*, **89**(3-4), 380-394. https://doi.org/10.1016/j.compstruc.2010.11.006

Chen, C.Q., Shi, Y., Zhang, Y.S., Zhu, J. and Yan, Y.J. (2006), "Size dependence of Young's modulus in ZnO nanowires", *Phys. Rev. Lett.*, **96**(7), 075505. https://doi.org/10.1103/PhysRevLett.96.075505

Chu, L., Shi, J. and Souza de Cursi, E. (2018), "Vibration analysis of vacancy defected graphene sheets by monte carlo based finite element method", *Nanomaterials*, **8**(7), 489. https://doi.org/10.3390/nano8070489

Compagnini, G., Giannazzo, F., Sonde, S., Raineri, V. and Rimini, E. (2009), "Ion irradiation and defect formation in single layer graphene", *Carbon*, **47**(14), 3201-3207. https://doi.org/10.1016/j.carbon.2009.07.033

Dastjerdi, S., Lot, M. and Jabbarzadeh, M. (2016), "The effect of vacant defect on bending analysis of graphene sheets based on the Mindlin nonlocal elasticity theory", *Compos. Part B Eng.*, **98**(1), 78-87. https://doi.org/10.1016/j.compositesb.2016.05.009

Eringen, A.C. (1983), "On differential equations of nonlocal elasticity and solutions of screw dislocation and surface waves", *J. Appl. Phys*, **54**, 4703-4710. https://doi.org/10.1063/1.332803

Fadaee, M. (2016), "Buckling analysis of a defective annular graphene sheet in elastic medium", *Appl. Math. Model*, **40**(3), 1863-1872. https://doi.org/10.1016/j.apm.2015.09.029

Guo, Y., Ruess, M. and Gürdal, Z. (2014), "A contact extended isogeometric layerwise approach for the buckling analysis of delaminated composites", *Compos. Struct.*, **116**(1), 55-66. https://doi.org/10.1016/j.compstruct.2014.05.006

Hassan, M., Marin, M., Ellahi, R. and Alamri, S.Z. (2018), "Exploration of convective heat transfer and flow characteristics synthesis by Cu-Ag/water hybrid-nanofluids", *Heat Transf. Res.*, **49**(18), 1837-1848. https://doi.org/10.1615/HeatTransRes.2018025569

Hosseini, S.M. and Zhang, C. (2018), "Elastodynamic and wave propagation analysis in a FG Graphene platelets-reinforced nanocomposite cylinder using a modified nonlinear micromechanical model", *Steel Compos. Struct., Int. J.*, **27**(3), 255-271. https://doi.org/10.12989/scs.2018.27.3.255

Hosseini Hashemi, S., Mehrabani, H. and Ahmadi-Savadkoohi, A. (2015), "Exact solution for free vibration of coupled double viscoelastic graphene sheets by visco pasternak medium", *Compos. Part B-Eng.*, **78**, 377-383. https://doi.org/10.1016/j.compositesb.2015.04.008

Hughes, T.J.R., Cottrell, J.A. and Bazilevs, Y. (2005), "Isogeometric analysis: CAD, finite elements, NURBS, exact geometry and mesh refinement", *Comput. Methods Appl. Mech. Eng.*, **194**(39-41), 4135-4195. https://doi.org/10.1016/j.cma.2004.10.008

Javani, R., Bidgoli, M.R. and Kolahchi, R. (2019), "Buckling analysis of plates reinforced by Graphene platelet based on Halpin-Tsai and Reddy theories", *Steel Compos. Struct., Int. J.*, **31**(4), 419-426. https://doi.org/10.12989/scs.2019.31.4.419

Kapoor, H. and Kapania, R. (2012), "Geometrically nonlinear NURBS isogeometric finite element analysis of laminated composite plates", *Compos. Struct.*, **94**(12), 3434-3447. https://doi.org/10.1016/j.compstruct.2012.04.028

Karami, B., Janghorban, M. and Tounsi, A. (2017), "Effects of triaxial magnetic field on the anisotropic nanoplates", *Steel Compos. Struct., Int. J.*, **25**(3), 361-374. https://doi.org/10.12989/scs.2017.25.3.361

Karami, B., Janghorban, M., Shahsavari, D. and Touns, A. (2018a), "A size-dependent quasi-3D model for wave dispersion analysis of FG nanoplates", *Steel Compos. Struct., Int. J.*, **28**(1), 99-110. https://doi.org/10.12989/scs.2018.28.1.099

Karami, B., Janghorban, M. and Tounsi, A. (2018b), "Nonlocal strain gradient 3D elasticity theory for anisotropic spherical nanoparticles", *Steel Compos. Struct., Int. J.*, **27**(2), 201-216. https://doi.org/10.12989/scs.2018.27.2.201

Kiendl, J., Bletzinger, K.U., Linhard, J. and Wuchner, R. (2009), "Isogeometric shell analysis with Kirchhoff-Love elements", *Comput. Method Appl. M.*, **198**(49-52), 3902-3914. https://doi.org/10.1016/j.cma.2009.08.013

Kim, H.J., Seo, Y.D. and Youn, S.K. (2010), "Isogeometric analysis with trimming technique for problems of arbitrary complex topology", *Comput. Methods Appl. Mech. Engrg.*, **199**(45-48), 2796-2812. https://doi.org/10.1016/j.cma.2010.04.015

Kitipornchai, S., He, X.Q. and Liew, K.M. (2005), "Continuum model for the vibration of multilayered graphene sheets", *Phys. Rev. B.*, **72**(7), 075443. https://doi.org/10.1103/PhysRevB.72.075443

Kumar, D. and Srivastava, A. (2016), "Elastic properties of CNT- and Graphene-reinforced nanocomposites using RVE", *Steel Compos. Struct., Int. J.*, **21**(5), 1085-1103. https://doi.org/10.12989/scs.2016.21.5.1085

Kuzhir, P., Volynets, N., Maksimenko, S., Kaplas, T. and Svirko, Y. (2013), "Multilayered graphene in Ka-band: Nanoscale coating for aerospace applications", *J. Nanosci. Nanotechnol.*, **13**(8), 5864-5867. https://doi.org/10.1166/jnn.2013.7551

Lam, D.C.C., Yang, F., Chong, A.C.M., Wang, J. and Tong, P. (2003), "Experiments and theory in strain gradient elasticity", *J. Mech. Phys. Solids*, **51**(8), 1477-1508. https://doi.org/10.1016/S0022-5096(03)00053-X

Le-Manh, T. and Lee, J. (2014), "Postbuckling of laminated composite plates using NURBS-based isogeometric analysis", *Compos. Struct.*, **109**, 286-293. https://doi.org/10.1016/j.compstruct.2013.11.011

Le-Manh, T., Luu-Anh, T. and Lee, J. (2016), "Isogeometric analysis for flexural behavior of composite plates considering large deformation with small rotations", *Mech. Adv. Mater. Struct.*, **23**(3), 328-336. https://doi.org/10.1080/15376494.2014.981616

Lim, C.W.W., Zhang, G. and Reddy, J.N. (2015), "A higher-order nonlocal elasticity and strain gradient theory and its applications in wave propagation", *J. Mech. Phys. Solids*, **78**, 298-313. https://doi.org/10.1016/j.jmps.2015.02.001

Liu, G.R. (2003), *Meshfree Methods: Moving Beyond the Finite Element Method*, CRC Press, USA.

Liu, G.R. and Chen, X.L. (2001), "A mesh-free method for static and free vibration analyses of thin plates of complicated shape", *J. Sound Vib.*, **241**(5), 839-855. https://doi.org/10.1006/jsvi.2000.3330

Malagu, M., Benvenuti, E. and Simone, A. (2012), "A finite element and b-spline methods for one-dimensional non-local elasticity", In: *ECCOMAS 2012: 6th European Congress on computational methods in applied sciences and engineering*, Vienna University of Technology, Vienna, Austria, September.

Marin, M. (1994), "The Lagrange identity method in thermoelasticity of bodies with microstructure", *Int. J. Eng. Sci.*, **32**(8), 1229-1240. https://doi.org/10.1016/0020-7225(94)90034-5

Marin, M. (1999), "An evolutionary equation in thermoelasticity of dipolar bodies", *J. Math. Phys.*, **40**(3), 1391-1399. https://doi.org/10.1063/1.532809

Marin, M. and Craciun, E.M. (2017), "Uniqueness results for a boundary value problem in dipolar thermoelasticity to model composite materials", *Compos. Part B-Eng.*, **126**, 27-37. https://doi.org/10.1016/j.compositesb.2017.05.063

Marina, P.E., Ali, G.A.M., See, L.M., Teo, E.Y.L., Ng, E.P. and Chong, K.F. (2016), "In situ growth of redox-active iron-centered nanoparticles on graphene sheets for specific capacitance enhancement", *Arab. J. Chem.* https://doi.org/10.1016/j.arabjc.2016.02.006

Martinez-Asencio, J. and Caturla, M.J. (2015), "Molecular dynamics simulations of defect production in graphene by carbon irradiation", *Nucl. Instruments Methods Phys. Res. Sect. B Beam Interact with Mater. Atoms*, **352**, 225-228. https://doi.org/10.1016/j.nimb.2014.12.010

Mirakhory, M., Khatibi, M.M. and Sadeghzadeh, S. (2018), "Vibration analysis of defected and pristine triangular single-layer graphene nanosheets", *Curr. Appl. Phys.*, **18**(11), 1327-1337. https://doi.org/10.1016/j.cap.2018.07.014

Mirzaei, M. and Kiani, Y. (2017), "Isogeometric Thermal buckling Analysis of Temperature Dependent FG Graphene Reinforced Laminated Plates using NURBS Formulation", *Compos. Struct.*, **180**, 606-616. https://doi.org/10.1016/j.compstruct.2017.08.057

Moradi-Dastjerdi, R. and Behdinan, K. (2019), "Thermoelastic static and vibrational behaviors of nanocomposite thick cylinders reinforced with Graphene", *Steel Compos. Struct., Int. J.*, **31**(5), 529-539. https://doi.org/10.12989/scs.2019.31.5.529

Nguyen, N.T., Hui, D., Lee, J. and Nguyen-Xuan, H. (2015), "An efficient computational approach for size-dependent analysis of functionally graded nanoplates", *Comput. Methods Appl. Mech. Engrg.*, **297**, 191-218. https://doi.org/10.1016/j.cma.2015.07.021

Norouzzadeh, A. and Ansari, R. (2018), "Isogeometric vibration analysis of functionally graded nanoplates with the consideration of nonlocal and surface effects", *Thin-Wall. Struct.*, **127**, 354-372. https://doi.org/10.1016/j.tws.2017.11.040

Othman, I.A. and Marin, M. (2017), "Effect of thermal loading due to laser pulse on thermoelastic porous medium under G-N theory", *Results Phys*., **7**, 3863-3872. https://doi.org/10.1016/j.rinp.2017.10.012

Piegl, L. and Tiller, W. (1997), *The NURBS Book*, (Monographs in Visual Communication), Springer-Verlag, New York, USA.

Pradhan, S.C. and Kumar, A. (2010), "Vibration analysis of orthotropic graphene sheets using nonlocal elasticity theory and differential quadrature method", *Compos. Struct*., **93**(2), 774-779. https://doi.org/10.1016/j.compstruct.2010.08.004

Rajasekaran, G., Narayanan, P. and Parashar, A. (2016), "Effect of point and line defects on mechanical and thermal properties of graphene", *Crit. Rev. Solid State Mater. Sci*., **41**(1), 47-71. https://doi.org/10.1080/10408436.2015.1068160

Ribeiro, P. and Chuaqui, T.R.C. (2019), "Non-linear modes of vibration of single-layer non-local graphene sheets", *Int. J. Mech. Sci*., **150**, 727-743. https://doi.org/10.1016/j.ijmecsci.2018.10.068

Roh, H.Y. and Cho, M. (2004), "The application of geometrically exact shell elements to B-spline surfaces", *Comput. Method Appl. M*., **193**(23-26), 2261-2299. https://doi.org/10.1016/j.cma.2004.01.019

Rouhi, S. and Ansari, R. (2012), "Atomistic finite element model for axial buckling and vibration analysis of single-layered graphene sheets", *Phys. E. Low-Dimensional Syst. Nanostruct*., **44**(4), 764-772. https://doi.org/10.1016/j.physe.2011.11.020

Sadeghi, M. and Naghdabadi, R. (2010), "Nonlinear vibrational analysis of single-layer graphene sheets", *Nanotechnology*, **21**(10), 105705. https://doi.org/10.1088/0957-4484/21/10/105705

Sakhaee-Pour, A. (2009), "Elastic buckling of single-layered graphene sheet", *Comput. Mater. Sci*., **45**(2), 266-270. https://doi.org/10.1016/j.commatsci.2008.09.024

Sakhaee-Pour, A., Ahmadian, M.T. and Naghdabadi, R. (2008), "Vibrational analysis of single-layered graphene sheets", *Nanotechnology*, **19**(8), 85702. https://doi.org/10.1088/0957-4484/19/8/085702

Shahsavari, D., Karami, B. and Li, L. (2018), "A high-order gradient model for wave propagation analysis of porous FG nanoplates", *Steel Compos. Struct., Int. J*., **29**(1), 53-66. https://doi.org/10.12989/scs.2018.29.1.053

Siddique, J.A., Attia, N.F. and Geckeler, K.E. (2015), "Polymer nanoparticles as a tool for the exfoliation of graphene sheets", *Mater. Lett*., **158**(1), 186-189. https://doi.org/10.1016/j.matlet.2015.05.134

Sobhy, M. (2014), "Thermomechanical bending and free vibration of single-layered graphene sheets embedded in an elastic medium", *Phys. E. Low-Dimens. Syst. Nanostruct*., **56**, 400-409. https://doi.org/10.1016/j.physe.2013.10.017

Soleimani, A., Naei, M.H. and Mashhadi, M.M. (2017), "Buckling analysis of graphene sheets using nonlocal isogeometric finite element method for NEMS applications", *Microsyst. Technol*., **23**(7), 2859-2871. https://doi.org/10.1007/s00542-016-3098-6

Soleimani A., Dastani, K., Hadi, A. and Naei, M.H. (2019), "Effect of out-of-plane defects on the postbuckling behavior of Graphene sheets based on nonlocal elasticity theory", *Steel Compos. Struct., Int. J*., **30**(6), 517-534. https://doi.org/10.12989/scs.2019.30.6.517

Song, M., Kitipornchai, S. and Yang, J. (2017), "Free and forced vibrations of functionally graded polymer composite plates reinforced with graphene nanoplatelets", *Compos. Struct*., **159**, 579-588. https://doi.org/10.1016/j.compstruct.2016.09.070

Stan, G., Ciobanu, C.V., Parthangal, P.M. and Cook, R.F. (2007), "Diameter-dependent radial and tangential elastic moduli of ZnO nanowires", *Nano Letters*, **7**(12), 3691-3697. https://doi.org/10.1021/nl071986e

Sun, S., Wang, C., Chen, M. and Zheng, J. (2013), "A novel method to control atomic defects in graphene sheets by selective surface reactions", *Appl. Surf. Sci*., **283**, 566-570. https://doi.org/10.1016/j.apsusc.2013.06.146

Tasis, D., Papagelis, K., Spiliopoulos, P. and Galiotis, C. (2013), "Efficient exfoliation of graphene sheets in binary solvents", *Mater. Lett*., **94**, 47-50. https://doi.org/10.1016/j.matlet.2012.12.027

Thai, C.H., Nguyen-Xuan, H., Nguyen-Thanh, N., Le, T.H., Nguyen-Thoi, T. and Rabczuk, T. (2012), "Static, free vibration, and buckling analysis of laminated composite Reissner-Mindlin plates using NURBS-based isogeometric approach", *Int. J. Numer. Methods Eng*., **91**, 571-603. https://doi.org/10.1002/nme.4282

Tornabene, F., Fantuzzi, N., Ubertini, F. and Viola, E. (2015), "Strong formulation finite element method based on differential quadrature: a survey", *Appl. Mech. Rev*., **67**(2), 1-55. https://doi.org/10.1115/1.4028859

Tornabene, F., Bacciocchi, M., Fantuzzi, N. and Reddy, J.N. (2018), "Multiscale approach for three-phase CNT/polymer/ fiber laminated nanocomposite structures", *Polym. Compos*., **40**(S1), E102-E126. https://doi.org/10.1002/pc.24520

Tran, L.V., Lee, J., Nguyen-Van, H., Nguyen-Xuan, H. and Wahab, M.A. (2015), "Geometrically nonlinear isogeometric analysis of laminated composite plates based on higher-order shear deformation theory", *Int. J. Non-Linear Mech*., **72**, 42-52. https://doi.org/10.1016/j.ijnonlinmec.2015.02.007

Tran, L.V., Phung-Van, P., Lee, J., Wahab, M.A. and Nguyen-Xuan, H. (2016), "Isogeometric analysis for nonlinear thermomechanical stability of functionally graded plates", *Compos. Struct*., **140**, 655-667. https://doi.org/10.1016/j.compstruct.2016.01.001

Wang, X., Zhu, X. and Hu, P. (2015), "Isogeometric finite element method for buckling analysis of generally laminated composite beams with different boundary conditions", *Int. J. Mech. Sci*., **104**, 190-199. https://doi.org/10.1016/j.ijmecsci.2015.10.008

Wei, Y., Wang, B., Wu, J., Yang, R. and Dunn, M.L. (2012), "Bending rigidity and Gaussian bending stiffness of single-layered graphene", *Nano Lett*., **13**(1), 26-30. https://doi.org/10.1021/nl303168w

Yang, F., Chong, A.C.M., Lam, D.C.C. and Tong, P. (2002), "Couple stress based strain gradient theory for elasticity", *Int. J. Solids Struct*., **39**(10), 2731-2743. https://doi.org/10.1016/S0020-7683(02)00152-X

Yu, T.T., Yin, S., Bui, T.Q. and Hirose, S. (2015), "A simple FSDT-based isogeometric analysis for geometrically nonlinear analysis of functionally graded plates", *Finite Elem. Anal. Des*., **96**, 1-10. https://doi.org/10.1016/j.finel.2014.11.003

Zhang, Y., Lei, Z.X., Zhang, L.W., Liew, K.M. and Yu, J.L. (2015), "Engineering Analysis with Boundary Elements Nonlocal continuum model for vibration of single-layered graphene sheets based on the element-free kp-Ritz method", *Eng. Anal. Bound. Elem*., **56**, 90-97. https://doi.org/10.1016/j.enganabound.2015.01.020

CC